

Observation of variation in γ -ray flux during the total solar eclipse at Siliguri (India) after developing a RooFit-based model

Pranaba K Nayak^{a,*}, A Bhadra^c, S Das^b, SR Dugad^a, SK Ghosh^b, D Gupta^b, SK Gupta^a, A Jain^a, I Mazumdar^a, PK Mohanty^a, S Raha^b, SK Saha^b and S Singh^b

^aTata Institute of Fundamental Research, 1, Homi Bhabha Road, Mumbai 400005, India

^bBose Institute, Department, University, Sector V, Block – EN, Salt Lake, Kolkata 700 091, India

^cCenter for High Energy and Cosmic ray Physics, North Bengal University, Siliguri 734 013, India

E-mail: pranaba@hotmail.com, aru_bhadra@yahoo.com, supdas@gmail.com, shashi.dugad@gmail.com, sanjay_k_ghosh@yahoo.co.in, dhruba@jcbose.ac.in, gupta.crl@gmail.com, atul@crl.tifr.res.in, indramazumdar@gmail.com, pravata2006@gmail.com, sibajiraha@gmail.com, swapan@jcbose.ac.in, 2006.sumana@gmail.com

The variability in γ -ray flux observed during total solar eclipses holds significant scientific interest. For our study, we employed two large-volume sodium iodide detectors to measure the γ -ray flux before, during, and after the "eclipse of the century" on 22 July 2009, visible from India. Analyzing the acquired spectra proved challenging due to the fluctuating levels of radon daughters. Furthermore, the presence of rain during the eclipse added further complexity to the analysis. To address these issues, we developed a RooFit-based method. Our newly devised model combines two exponential functions with 12 Gaussian functions representing the dominant γ -ray lines, enabling the generation of a comprehensive compound energy spectrum. We successfully demonstrated the effectiveness of this model in fitting individual spectra of various time durations, irrespective of rain or time, and its potential to isolate the influence of rain. Upon re-evaluating the Siliguri data, we observed a notable reduction in the variability of γ -ray flux. ROOFit was used successfully for the first time to the background γ -ray spectrum without considering detector parameters.

*38th International Cosmic Ray Conference (ICRC2023)
26 July - 3 August, 2023
Nagoya, Japan*



^{*}Speaker

© Copyright owned by the author(s) under the terms of the Creative Commons Attribution-NonCommercial-NoDerivatives 4.0 International License (CC BY-NC-ND 4.0).

<https://pos.sissa.it/>

1 Introduction

During a total solar eclipse (TSE), there is a brief period when the Earth is shielded from the Sun's direct radiation [1-3]. This phenomenon can result in changes in the flux of γ -ray detected on the Earth's surface [2-6]. When the Sun is visible in the sky, γ -rays from the Sun can be seen on the Earth's surface. However, during a TSE, the Moon moves in front of the Sun, blocking its direct radiation and causing a decrease in the γ -ray flux. It is challenging to detect the reduction in the γ -ray flux during a TSE. However, it has been observed in some studies [1-5], and the effect is most noticeable within the range of a few MeVs [2-6]. One proposed explanation for the decrease in γ -ray flux during a TSE is the absorption of gamma rays by the Earth's atmosphere. The atmosphere acts as a shield, absorbing and scattering high-energy radiation before it reaches the ground [5-7]. During TSE, the Moon blocks the direct radiation from the Sun, creating a more direct line of sight between the γ -ray source and the Earth's surface. This can result in increased absorption of γ -rays by the atmosphere, decreasing the detected flux. Overall, the impact of a TSE on the γ -ray flux is an intriguing phenomenon that can be studied using advanced instruments and sophisticated techniques.

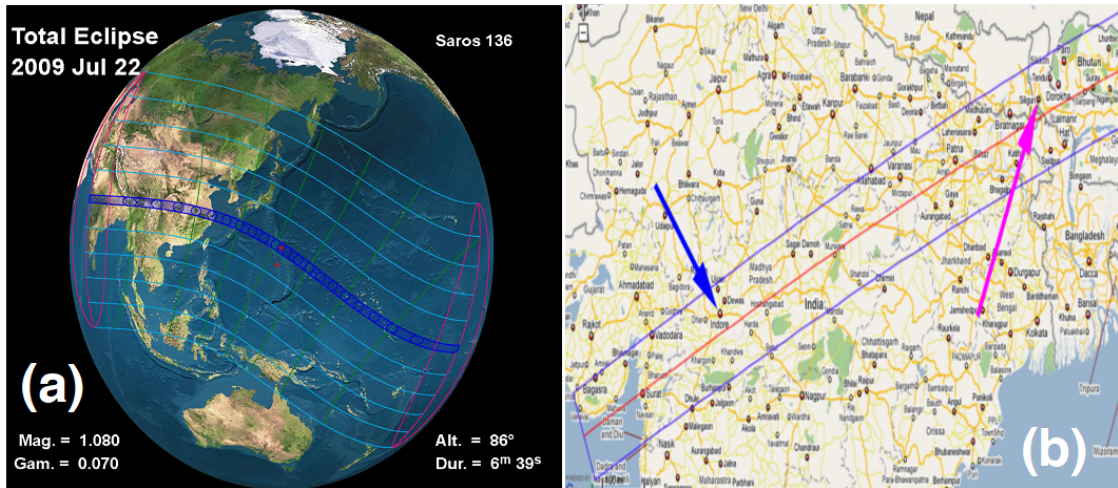


Figure 1: (a) Passage of the TSE on 22 July 2009 from the Arabian Sea to the mid Pacific Ocean is shown by a band, (b) The totality path in major parts of India with arrows indicating sites (blue for Indore and Pink for Siliguri) with identical experimental design.

Figure 1a displays the TSE that occurred on July 22, 2009, featuring an exceptionally long totality duration of 6 minutes and 39 seconds [3,5,6]. This eclipse was visible from a narrow corridor traversing the eastern hemisphere. The Moon's umbral shadow originated in the Arabian Sea and passed through India. The central line of the Moon's shadow commenced at 00:53 UTC in India's Bay of Cambay, with the eclipse track initially spanning 205 kilometers in width, as depicted in Figure 1b. Notable Indian cities, including Indore, Bhopal, Varanasi, Patna, Siliguri, and Dibrugarh, experienced the totality. Siliguri (Latitude: 26.71 N; Longitude: 88.41 E; altitude: 122m asl) with eclipse magnitude 1.022. Siliguri was selected as one of the sites (the other is Indore) for the experiment due to its significantly extended totality of 227 seconds, improved transportation accessibility, and better infrastructure availability.

2. Experimental setup, calibration and data collection

In this study, two NaI(Tl) detectors with a hexagonal cross-section were utilized (shown in Figure 2a). Each detector had dimensions of 8.5 cm per side and a length of 25.4 cm. They were positioned face-to-face with a distance of 15.0 cm between their faces and a vertex-to-vertex distance of 16.8 cm. A 3-inch diameter photomultiplier (PMT; Hamamatsu-R1911) with a 10-stage dynode was employed to detect the emitted light. The PMT operated at a bias voltage of +800 V. Figure 2b illustrates the setup of the signal processing electronics. The signals from the dynodes of the PMT were directed to dedicated fixed-gain charge-sensitive pre-amplifiers, which were integrated with the PMT bases, as depicted in Figure 2c.

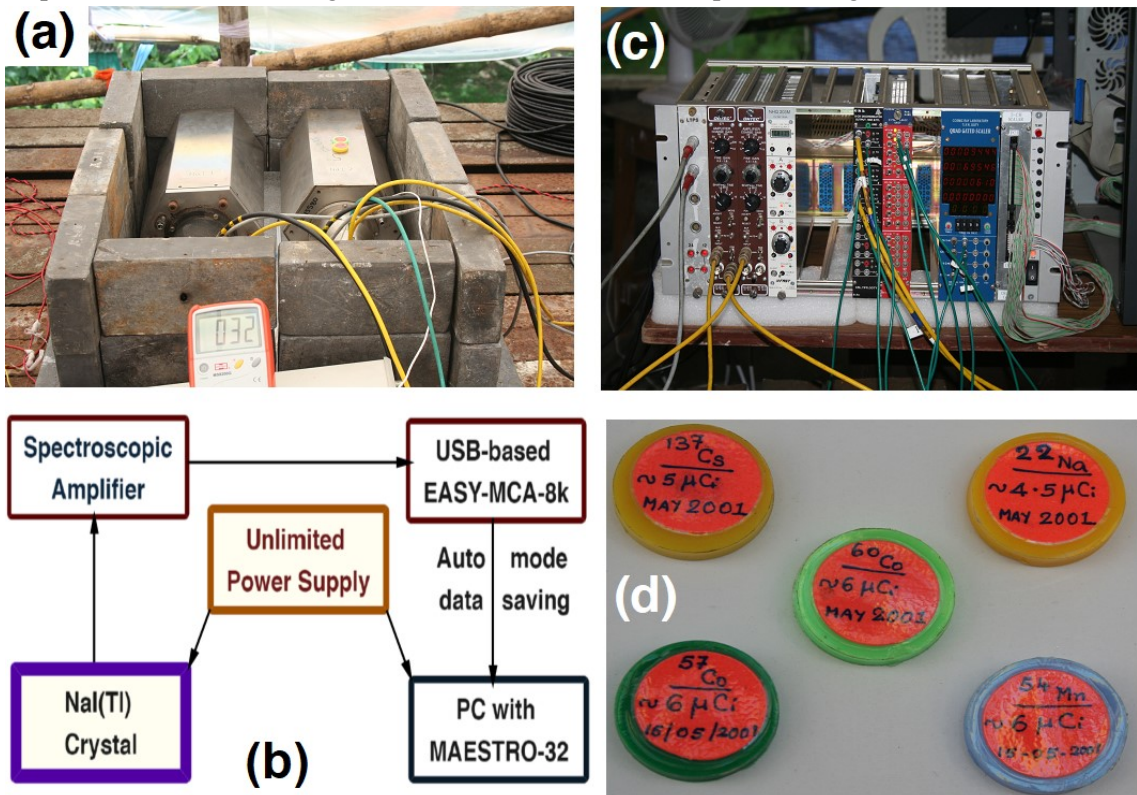


Figure 2: (a) NaI(Tl) detectors were housed within lead shielding, (b) A schematic diagram depicting the signal processing electronics for a detector, (c) An illustration of the arrangement of the associated electronics, and (d) Radioactive sources used for detector calibration.

These pre-amplifier signals were shaped and amplified using a programmable spectroscopy amplifier (CAEN N1568A, 16-channel). The amplified signals were digitized using two multi-channel analyzers (ORTEC EASY MCA-8k). Subsequently, the data was transferred to personal computers (PCs) via MAESTRO-32 software for further processing. The detectors underwent extensive calibration at regular intervals using standard γ -ray sources, as shown in Figure 2d. These sources included Cs137 (662 keV) and Co60 (1173 and 1332 keV), and the calibration was performed before and after the actual data collection period. These two detectors' energy resolutions were better than 8% at 662 keV and less than 7% at the energies of Co60. The peak-to-valley ratio for the 1332 keV peak (Co60) was approximately 10. To restrict the detector's dynamic range to 3800 keV, the gain of the spectroscopic amplifier was

appropriately adjusted. The gains were continuously monitored and cross-checked at regular intervals, and they were found to remain stable throughout the data collection. The data were collected without interruptions at a 60-second break, with provisions for further adjustments as required in later stages. The calibration of the system was found to remain stable during the continuous two-week data collection period. The gain changes for each spectral line varied within a few channels, corresponding to a single keV. For discussion, data from one of the detectors were considered.

3. Background spectra, their fitting and the outcome

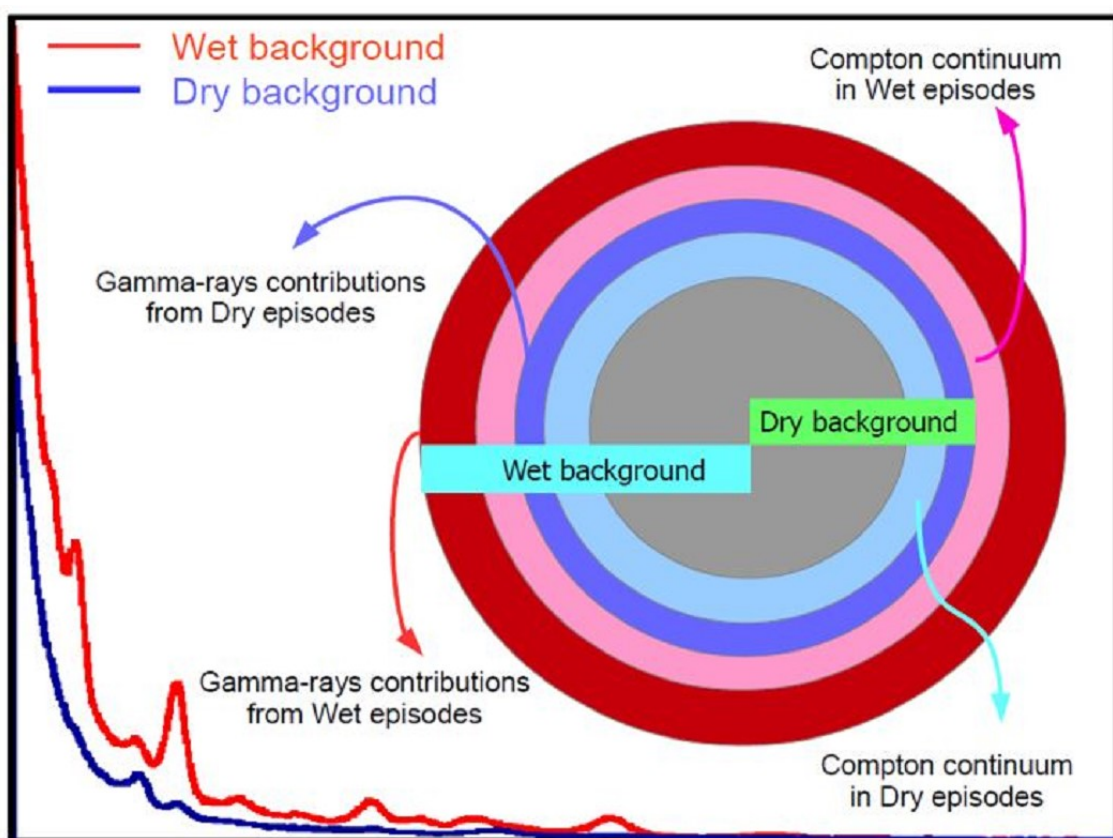


Figure 3: Understanding the true background.

The γ -ray background spectrum exhibits similar characteristics to the spectrum depicted in Figure 3 (shown on the extreme left side, in blue). It demonstrates a distinctive rapid decline in the low-energy region with a few peaks resulting from various γ -ray lines. As mentioned earlier, these lines, including K^{40} and Tl^{208} , primarily stem from surrounding concrete and construction materials [7-9]. Despite significant efforts to minimize terrestrial γ -ray contributions, it is impossible to eliminate them entirely. Moreover, this component becomes more critical during rainfall due to the appearance of additional γ -ray lines from Pb^{214} and Bi^{214} . Therefore, the key challenge lies in comprehensively understanding, efficiently analyzing, and meticulously isolating cosmic γ -ray components from compound spectra where the photo-peaks exhibit broad

Gaussian shapes. Interestingly, estimating the signal (in this case, cosmic γ -ray portion) in the presence of an unknown background (in this case, terrestrial γ -ray) may be less problematic, unlike the reverse situation [7, 8, 10]. To address this challenge, we utilized the statistical toolkit "RooFit," which simultaneously incorporates various statistical distributions to fit the recorded energy spectrum [11, 12]. Incorporating prior knowledge of the parameters obtained from actual experiments facilitates a better understanding and aids in designing an effective fitting procedure. Detailed information regarding the radioisotopes present (along with their respective emitted γ -rays) in the rain was obtained and extensively discussed in our earlier communication. In addition to K^{40} and Tl^{208} , it was discovered that the low-energy region exhibited three prominent γ -ray lines emitted by Pb^{214} at energies of 242, 295, and 352 keV. In the high-energy region above 500 keV, eight detectable γ -ray lines emitted by Bi^{214} were observed at energies of 609, 768, 934, 1120, 1238, 1378, 1764, and 2204 keV. Further comprehensive details regarding these isotopes and their relative abundances corresponding to γ -ray lines can be found in other sources. It has long been observed that ultra-low-level background spectra contain an additional line at 511 keV originating from Na^{22} , especially when using high-sensitivity detectors. In fact, we observed the 511 keV lines in all the recorded spectra.

Following the aforementioned steps, we attempted to fit the four-hour data without rain episodes, similar to the blue line shown in Figure 3. The overall profile of the background consists of the sum of Compton scattering of photons from all γ -ray lines and the terrestrial gamma-ray (TGR) background originating from the surrounding materials. To achieve an improved quality of fitting and a better description of the TGR background, as explained in our earlier communication, the continuum background was fitted with two exponential functions in addition to 14 Gaussian functions. A total of 14 Gaussian functions were generated, representing three γ -ray lines from Pb^{214} , eight from Bi^{214} , and one each from Na^{22} , K^{40} , and Tl^{208} , respectively.

Using appropriate RooFit functions, two sets of compound probability density functions (pdfs) were generated for Pb^{214} and Bi^{214} lines. These pdfs were combined with the three pdfs for Na^{22} , K^{40} , and Tl^{208} , resulting in a combined Gaussian profile. For individual radioisotopes, the peak positions and widths of γ -ray lines were determined from calibration and preliminary runs. During the analysis, these parameters were then fixed along with their respective branching ratios. In the next step, two exponential pdfs were generated independently without predefined initial constraints. These exponential pdfs were then combined to form a combined exponential portion. Finally, the Gaussian and exponential contributions were added to obtain a single compound energy spectrum representing the fit to the measured data within the RooFit framework. The above parameterization to reproduce the TGR background appears to have worked reasonably well and was found relatively easy to be implemented. While using the above parameterization, the amount or duration of rainfall or the delay in measuring the γ -ray activity is not required and was not considered in the present analysis.

4. True background, the methodology and its isolation

All the data sets collected at the site can be called the "raw background." In the absence of rain, the spectrum exhibits a falling γ -ray distribution, as depicted by the blue solid line in Figure 3. However, the spectrum changes shape during heavy rainfall, resembling the red solid line. This modified spectrum during rain can be called the "wet background," which includes additional contributions due to the presence of rain. The Venn diagram inset illustrates that the "dry background" encompasses contributions from γ -ray lines and the resulting Compton continuum background. Similarly, the "wet episodes" include contributions from γ -rays and the Compton continuum and all the factors contributing to the "dry background." Therefore, our primary objective is to separate the "true background" from all other forms of terrestrial background. To achieve this, it was crucial to develop a method that isolates the γ -ray lines and discerns the respective Compton continuum contributions. Considering the short decay lifetimes of 26.8 minutes for Pb^{214} and 19.9 minutes for Bi^{214} , it is reasonable to assume that virtually all radioisotopes would have decayed after four hours. Thus, any period beyond four hours of rain can be considered a "dry period."

It should be noted that the TGR background level typically does not change significantly over one hour, except in drastic changes in radon and its decay products. However, to avoid potential complications arising from variable rain episodes, only those four-hour periods were designated as "dry periods" if they were preceded by at least a minimum of four consecutive dry hours and had no observed rain during that particular four-hour period. Initially, data collected from the 19th of July onwards was integrated over a four-hour duration and assigned as either a "dry episode" or a "wet episode," depending on the occurrence of rain. The episodes with a break for calibration or any instrumental changes were not considered. Rainfall was found to significantly enhance the "raw background." Dry periods were defined as periods with no rain observed for four consecutive hours and during the preceding four hours.

For dry episodes, total calculated counts from the episode can be defined as:

$\Sigma_{\text{Dry}_i} = \Sigma_{\text{DryEx}} + \Sigma_{\text{dryGs}}$, where Σ_{Dry_i} is the sum of the exponential portion (Σ_{DryEx}) and Gaussian portion (Σ_{dryGs}). Similarly, for wet episodes, total calculated counts from the episode can be defined as: $\Sigma_{\text{Wet}_i} = \Sigma_{\text{WetEx}} + \Sigma_{\text{wetGs}}$, where Σ_{Wet_i} is the sum of the exponential portion (Σ_{WetEx}) and Gaussian portion (Σ_{wetGs}). The excess exponential (ExEx) and excess Gaussian (ExGs) portions were obtained for individual four-hour time duration by subtracting their values from the preceding immediate dry period as: $\text{ExEx} = \Sigma_{\text{WetEx}} - \Sigma_{\text{DryEx}}$; and $\text{ExGs} = \Sigma_{\text{WetEx}} - \Sigma_{\text{dryEx}}$. Subsequently, individual values for each excess exponential and excess Gaussian portion, plotted in Figure 4(a), and the corresponding linear fitted values were obtained.

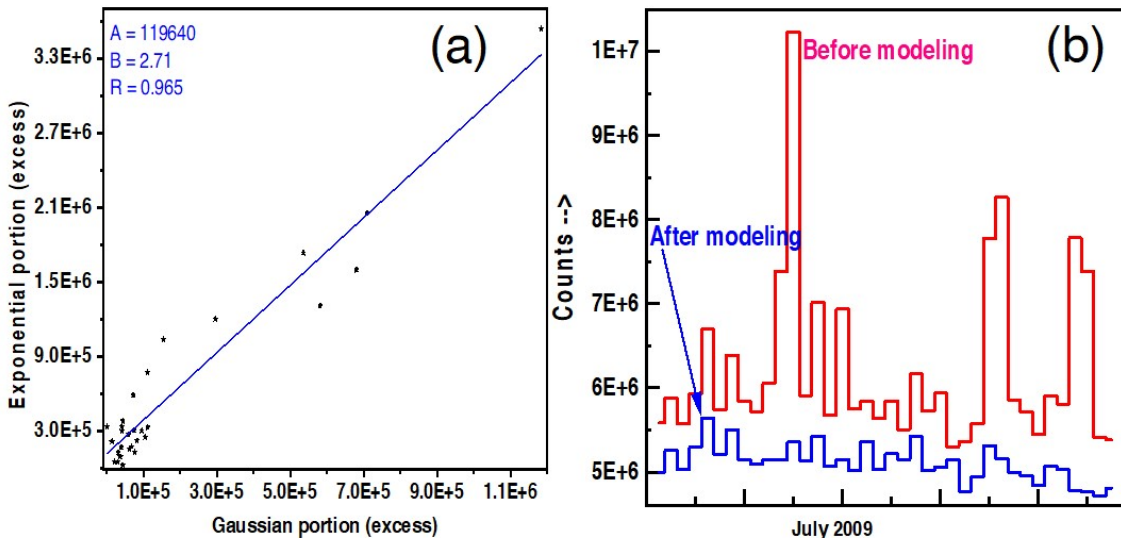


Figure 4: (a) Calibration curve obtained for data with four-hour duration, (b) The improvement after rain-affected four-hourly long term data modeling.

Accordingly, the obtained excess Gaussian portions ($ExEx_i$) were converted to corresponding exponential portions (excess exponential due to Gaussian contribution), to obtain true background as follows: True background = $\Sigma Ex_i - ExEx_i$; where ΣEx_i is the total exponential portion for each duration obtained after fitting. The true background obtained by the above method for the period 19th July to 28th July has been calculated and was plotted along with the raw background data (in the red solid histogram) in Figure 4(a), whereas the true background (blue solid histogram) became flat for the above period, irrespective of quantum of rainfall.

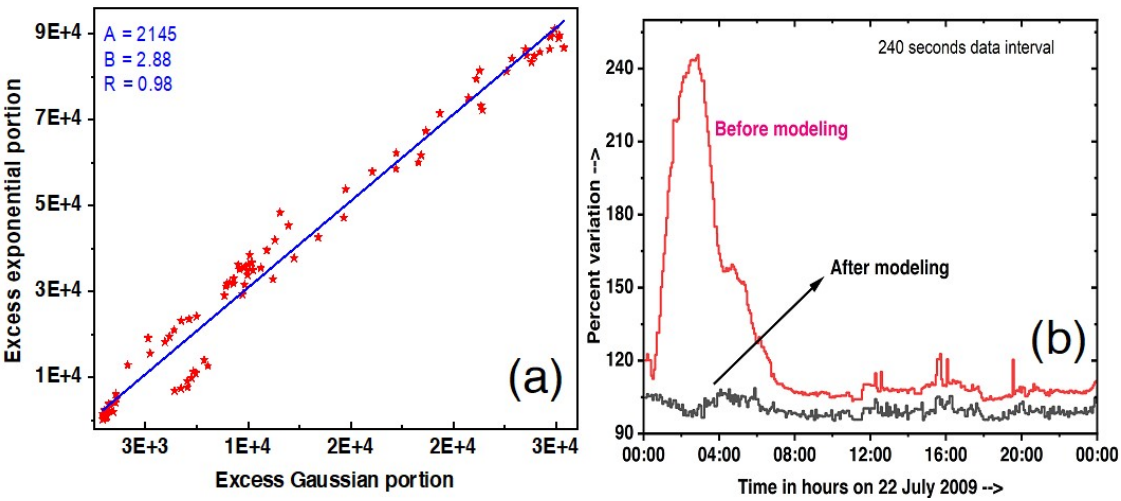


Figure 5: (a) Calibration curve obtained for four-minute duration data, (b) The improvement after modeling of rain-affected four-minute data on total solar eclipse day.

Following a similar strategy, data with four minutes duration was analysed, and calibration constant was obtained by plotting exponential excess versus Gaussian excess, as shown in Figure 5(a). The true background for the eclipse day was calculated and plotted in Figure 5(b), along with the raw background.

5. Summary and further scope

This is the first instant of simultaneous measurements at two different sites on the same total solar eclipse using identical sets of instruments. ROOFit is used successfully to the background γ -ray spectrum for the first time without considering detector parameters. The outcome will be compared with the results obtained from the same TSE experiment at Indore for a more profound understanding of the phenomena.

Acknowledgments: We thank Prof. G.B. Mohanty for his help with RooFit, Dr. C.C. Dey (SINP, Kolkata), and Dr. S. Bhattacharya (VECC, Kolkata) for crucial experimental components. This work was supported by the DAE (Project Identification No. RTI4002) and the DST (under IRHPA scheme No. IR/S2/PF-01/2003 of SERC) of the Government of India.

Author Contributions: Conceptualization: SKGupta, SR, IM, PKN; Methodology, software & formal analysis - PKN, SKGupta, IM, SRD, PKM; Validation: SD, SS, AB, PKN; Investigation: SR, SD, SKGhosh, DG, SS, AB, SKGupta, PKN, AJ; Resources: SR, AB, SKGhosh, SKS; Visualization & Writing original draft: PKN; Manuscript review & proofreading: All authors; Supervision, Project administration & Funding acquisition: SKGupta, SR, PKM, SRD.

References

- [1] P.K. Nayak *et al.*, *A study of the γ -ray flux during the total solar eclipse of 1 August 2008 at Novosibirsk, Russia*, *Astroparticle Physics*, **32** (2010) 286.
- [2] A. Bhaskar *et al.*, *A study of secondary cosmic ray flux variation during the annular eclipse of 15 January 2010 at Rameswaram, India*, *Astroparticle Physics* **35** (2011) 223.
- [3] T.A. Dallal *et al.*, *Solar Eclipse and Cosmic Ray Flux*, *Phys. Teacher*, **60** (2022) 100.
- [4] A. Pandya *et al.*, *A Variation in cosmic ray flux during Solar Eclipse on 21 June, 2020 at Jaipur, India*, *Astroparticle Physics* **136** (2022) 102659.
- [5] D.L. Chichester *et al.*, *Observation of natural background radiation during the Great American Eclipse*, *Appl. Radiat. Isotopes*, **142** (2018) 151.
- [6] R. Bhattacharya *et al.*, *Cosmic ray intensity and surface parameters during solar eclipse on 22 July 2009 at Kalyani in West Bengal*, *Curr. Sci.*, **98** (2010) 1609.
- [7] P.K. Nayak *et al.*, *Estimation of K, U and Th in Precambrian ores by low-level γ -ray spectroscopy*, *Ind. J. Phys.* **77 A** (2003) 503.
- [8] P.K. Nayak & V. Vijayan, *Complementary PIGE, PIXE, EDXRF and γ -ray spectroscopic investigation on natural chromites*, *Nucl. Instr. Meth. B*, **245** (2006) 505.
- [9] S. Roy *et al.*, *Interplay between eclipses and soft cosmic rays*, in proceedings of ICRC2021 PoS (ICRC2021) 131.
- [10] P.K. Nayak *et al.*, *Study of terrestrial γ -ray background in presence of variable radioactivity from rain water*, *Astroparticle Physics* **72** (2016) 55.
- [11] I. Antcheva *et al.*, *ROOT—A C++ framework for petabyte data storage, statistical analysis and visualization*, *Comp. Phys. Commun.*, **180** (2009) 2499.
- [12] W. Verkerke & D. Kirkby, *The RooFit toolkit for data modelling*, Proc. Conf. Computing in High Energy & Nuclear Phys., La Jolla, California (2003).